

## MODIFICATION OF AlSi21CuNi ALLOY BY FAST COOLED ALLOY WITH Al, B AND Ti

Tomasz Lipinski

University of Warmia and Mazury in Olsztyn, Poland  
tomekl@uwm.edu.pl

**Abstract.** One of the most common castings applied in industrial production is aluminum-silicon alloy (ca. 25 % Si). Non-modified Al-Si alloy is characterized by coarse-grained structure, responsible for its poor physicochemical properties. The mechanical properties of hyper-eutectic silumins can be improved through chemical modification as well as traditional or technological processing. Modification improves the mechanical properties of alloys through grain refinement. Thermal analysis has been used to characterize the solidification processes of Al-Si alloy. The technique has been given a lot of information not only about solidification Al-Si alloys, but about microstructure and mechanical properties, too. This study presents the results of modification of an AlSi21CuNi alloy with composition aluminium+boron+titanium in different ranges. The experiments were conducted following a factor design  $2^3$  for 3 independent variables. The influence of the analyzed modifiers on the microstructure and mechanical properties of the processed alloy was presented in graphs. The modification of a hyper-eutectic AlSi21CuNi alloy improved the alloy's properties. The results of the tests indicate that the mechanical properties of the modified alloy are determined by the components introduced to the alloy.

**Keywords:** Al-Si alloy, modification, mechanical properties, thermal analysis.

### Introduction

Hyper-eutectic silumins are a popular group of casting alloys owing to their relatively low price, low melting temperature, high resistance to corrosion and high strength relative to specific gravity. Those attributes have contributed to the wide use of hyper-eutectic silumins in aviation, motor and ship building industries, first of all on the pistons for combustion engines.

The microstructure of unmodified AlSi21CuNi alloys comprises large grain primary beta phase and eutectic alpha and beta phase crystals. This composition is responsible for the alloy's low strength parameters, and it limits the extent of practical applications [1; 2].

The mechanical properties of hyper-eutectic silumin can be improved, like that of all casting alloys [3; 4], through modification or processing [5-13]. In the majority of cases alloys are modified to change the form and size of grains, mostly silicon grains, which reduces the interphase spacing of eutectic ( $\alpha + \beta$ ) and reducing the size of the primary beta phase [1]. This process causes changes in thermal effects of cooling alloy. The results of the study [1; 5; 11-16] indicate that the reaction's thermal effects as a solidification process influences the quality of the modification process, leading to changes in the microstructure and mechanical properties of the alloy.

There is a shift of the eutectic temperature and the eutectic point due to modification, it is known from the literature [17-18]. The differences in modification effectiveness should be attributed mainly to the solidification process which can be analyzed also by the thermal effects of the modification process.

In view of the growing popularity of modified alloys, the aim of this study was to determine the mechanical properties of hyper-eutectic silumins AlSi21CuNi modified with fast cooled mixtures of aluminum, boron and titanium different range of components.

### Materials and methods

The experimental material was AlSi21CuNi alloy which was regarded as representative of hyper-eutectic silumins. The alloy was obtained from industrial piglets. The alloy was melted in an electric furnace, and the modification process was carried out with fast cooled AlTiB, Al3TiB and AlTi6B. The alloy was modified at a temperature of 800°C for 8 minutes. Cylindrical samples, 8 mm in diameter and 75 mm in length, were poured into a dry sand moulds. The cooling curves analysis has been performed by means of a CRYSTALDIGRAPH PC-4T2L ver. 4.42 measuring device, but Dynamic Scanning Calorimetry measurement by NEITSH DSC204 F1 Phoenix. Casts were removed from molds, and specimens were collected for mechanical tests. Hardness was determined by the Brinell method by applying a test load of 612.9 N to a ball with a diameter of 2.5 mm. The side

surface of the head of the specimen used in a static tensile test was ground to a depth of 2 mm. Three measurements were taken per sample (6 measurements per cast). All measurements were carried out according to standard PN-EN ISO 6506-1:2014-12 "Metallic materials. Brinell hardness test. Part 1: Testing methodology" in the HPO 250 hardness tester. The tensile stress test was performed on a specimen with a length-to-diameter ratio of 5:1 in the ZD-30 universal tensile tester. Ultimate tensile strength and percentage elongation were determined. A tensile strength test was performed on two samples,  $\phi$  6 mm, for each melting point, according to standard PN-EN 6892-1: 2010 "Metallic materials. Tensile testing. Part 1: Testing methodology at room temperature". Applying total factorial experiment ( $2^3$ ) for three independent variables (table 1). The equation (1) was introduced for received plan of investigations the figure of equation of regress.

$$\hat{y} = b_0 + b_1x_1 + b_2x_2 + b_3x_3 + b_{12}x_1x_2 + b_{13}x_1x_3 + b_{23}x_2x_3 + b_{123}x_1x_2x_3. \quad (1)$$

Table 1

Level of variables

Variable	Primary level, %	Range of changes, %	Higher level, %	Lower level, %
AlTiB	2	1	3	1
Al <sub>3</sub> TiB	2	1	3	1
AlTi <sub>6</sub> B	2	1	3	1

The results were analyzed mathematically, which enabled to formulate the factor equation for three variables, for the parameters studied, at the level of significance  $\alpha = 0.05$ . The adequacy of the above mathematical equation was verified using the Fischer criterion for  $p = 0.05$ .

### Results and discussion

The results of a tensile strength (UTS) of AlSi21CuNi alloy with modifier (Table 1) are shown at (2) and Fig. 1, percentage elongation (A) at (3) and Fig. 2 and Brinell hardness (HB) at (4) and Fig. 3.

Due to difficulties with representing functions for three independent variables, figure drawings for the obtained function were developed from the experimental design on the assumption that each of the analyzed modifier components was present at a stable higher (3 %) or lower (1 %) level while the share of the remaining two components varied. Based on this approach, six graphic forms were developed for three modifier components.

$$\widehat{UTS} = 184.875 + 7.625x_1 + 3.875x_2 + 10.625x_3 - 3.875x_1x_2 - 5.375x_2x_3, \quad (2)$$

$$\hat{A} = 2.0625 + 2.875x_1 + 0.6625x_3 - 0.1375x_1x_2 - 0.2125x_2x_3 - 0.1375x_1x_2x_3, \quad (3)$$

$$\widehat{HB} = 106 + 3.25x_3 + 1.75x_1x_2 + 1.75x_1x_3 - 2.5x_2x_3 - x_1x_2x_3, \quad (4)$$

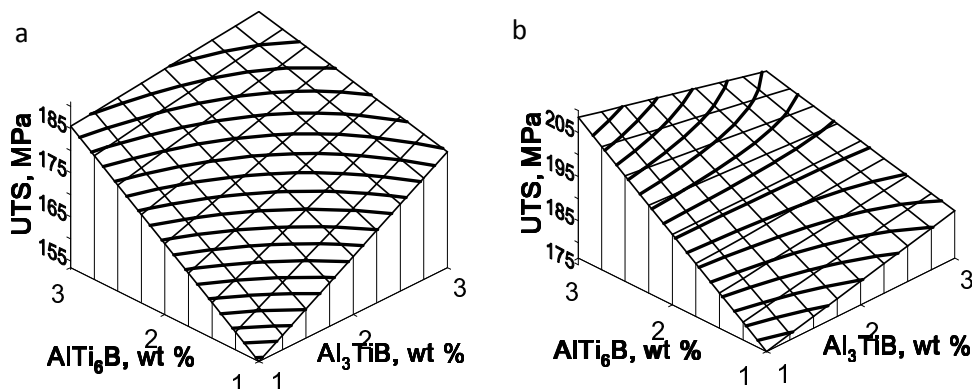


Fig. 1. The ultimate tensile strength (UTS) AlSi21CuNi alloy with:  
 a – Al<sub>3</sub>TiB ∈ <1, 3> (%) and AlTi<sub>6</sub>B ∈ <1, 3> (%) for AlTiB = 1 %;  
 b – Al<sub>3</sub>TiB ∈ <1, 3> (%) and AlTi<sub>6</sub>B ∈ <1, 3> (%) for AlTiB = 3 %

In an unmodified AlSi21CuNi alloy, ultimate tensile strength UTS was determined at 145 MPa, elongation A at 0.1 %, and Brinell hardness at 87 HB. Treatment with 1 % AlTiB + 1 % Al<sub>3</sub>TiB + 1 % AlTi<sub>6</sub>B a little increased ultimate tensile strength to 155 MPa and Brinell hardness to 105 HB. Elongation is the same. An increase in the AlTi<sub>6</sub>B content of the modifier to 3 % increased tensile strength by 30 MPa to 185 MPa (Fig. 1a), elongation by 2.9 % to 3.0 % (Fig. 2a) and hardness by 4 HB to 109 HB (Fig. 3a). An increase in the AlTiB content of the modifier to 3 % increased tensile strength by 25 MPa (by 65 MPa comparison to raw alloy) to 210 MPa (Fig. 1b), elongation by 1.3 % to 3.5 % (Fig. 2b) and decreased hardness to 108 HB (Fig. 3b). For all modifiers on higher level (Table 1) tensile strength is 196 MPa (Fig. 1b), elongation 2.7 % (Fig. 2b) and hardness 109 HB (Fig. 3b).

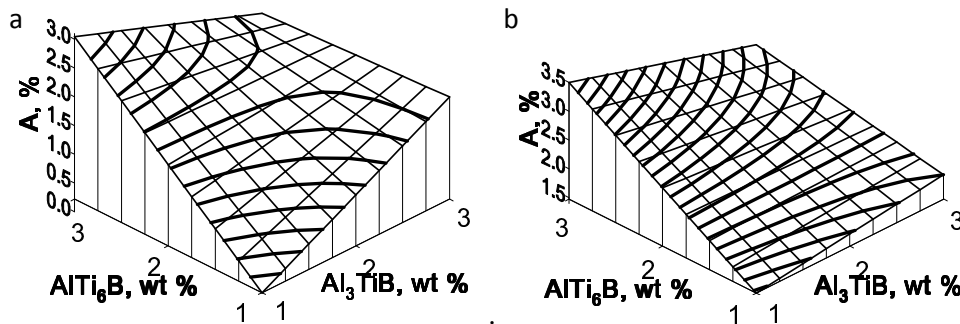


Fig. 2. Percentage elongation (A) AlSi21CuNi alloy with:

- a – Al<sub>3</sub>TiB ∈ <1, 3> (%) and AlTi<sub>6</sub>B ∈ <1, 3> (%) for AlTiB = 1 %;
- b – Al<sub>3</sub>TiB ∈ <1, 3> (%) and AlTi<sub>6</sub>B ∈ <1, 3> (%) for AlTiB = 3 %

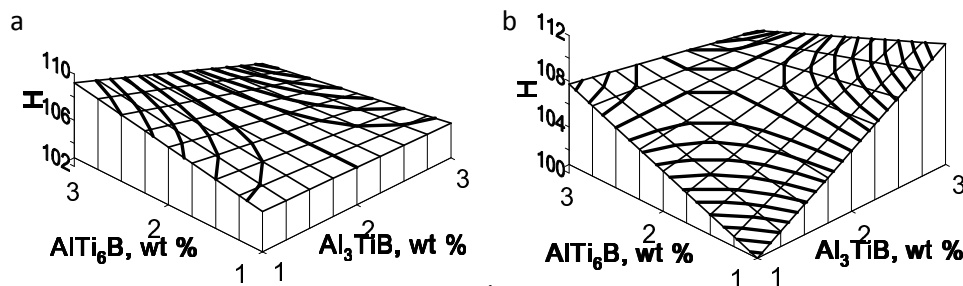


Fig. 3. Brinell hardness (HB) AlSi21CuNi alloy with:

- a – Al<sub>3</sub>TiB ∈ <1, 3> (%) and AlTi<sub>6</sub>B ∈ <1, 3> (%) for AlTiB = 1 %;
- b – Al<sub>3</sub>TiB ∈ <1, 3> (%) and AlTi<sub>6</sub>B ∈ <1, 3> (%) for AlTiB = 3 %

The microstructure of AlSi21CuNi silumin without modifying additives consists of a primary solid solution of aluminum in silicone (phase  $\beta$ ) and a solid solution of silicone in aluminum (phase  $\alpha$ ) (Fig. 1). Microstructure of AlSi21CuNi alloy with 3 % AlTiB + 1 % Al<sub>3</sub>TiB + 3 % AlTi<sub>6</sub>B (the best mechanical properties) is presented in Fig. 8. The a little refinement of primary dendrites of  $\beta$  phase was observed after all the processing of the AlSi21CuNi alloy in accordance to investigation plane (Table 1). The analyzed eutectic had a lamellar structure with a high degree of furcation.

Crystallization of hyper-eutectic AlSi21CuNi alloy with 3 % AlTiB + 1 % Al<sub>3</sub>TiB + 3 % AlTi<sub>6</sub>B by cooling curve and its time derivative are shown in Fig. 6. The derivative cooling curves provide more information about dynamic processes changes on the cooling curve. Its showed generation of energy for phase formation. The crystallization process consists of the formation of primary  $\beta$ -Si phase and next eutectic formation of Al-Si ( $\alpha + \beta$ ) eutectic during the last stage. The maximum thermal effect of  $\beta$  phase crystallization occurs at the B point, and eutectic ( $\alpha + \beta$ ) at the E point. Analysing the registered course of the cooling curve and its first derivative  $dT/dt$  the following points can be determined crystallization range: A-C for primary  $\beta$  phase and C-D eutectic ( $\alpha + \beta$ ). The time of holds of  $\beta$  phase and eutectic ( $\alpha + \beta$ ) are determine about dispersion of alloy, and then about its mechanical properties. If the holds time decreased, then size of phases decreased, too. Then the alloy has higher mechanical properties. The cooling curves and its first derivative is recorded in crystallizing alloys to the real times and scale, therefore represents the changes of energy on a macroscopic scale.

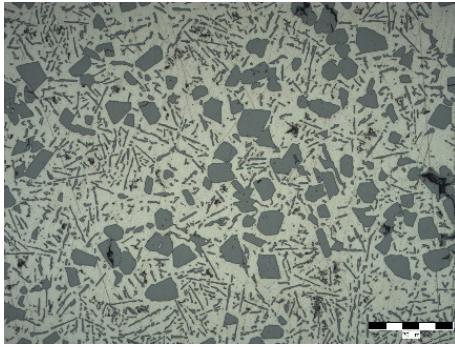


Fig. 4. Microstructure of the raw AlSi21CuNi alloy, etch. Mi8Al

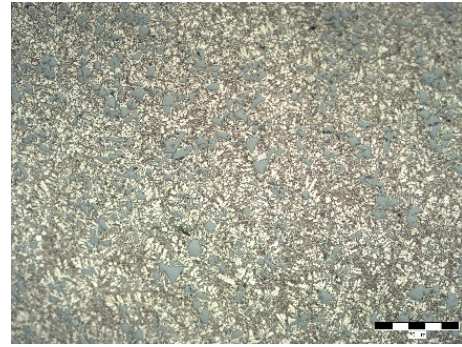


Fig. 5. Microstructure of AlSi21CuNi alloy with 3 % AlTiB + 1 % Al<sub>3</sub>TiB + 3 % AlTi<sub>6</sub>B, etch. Mi8Al

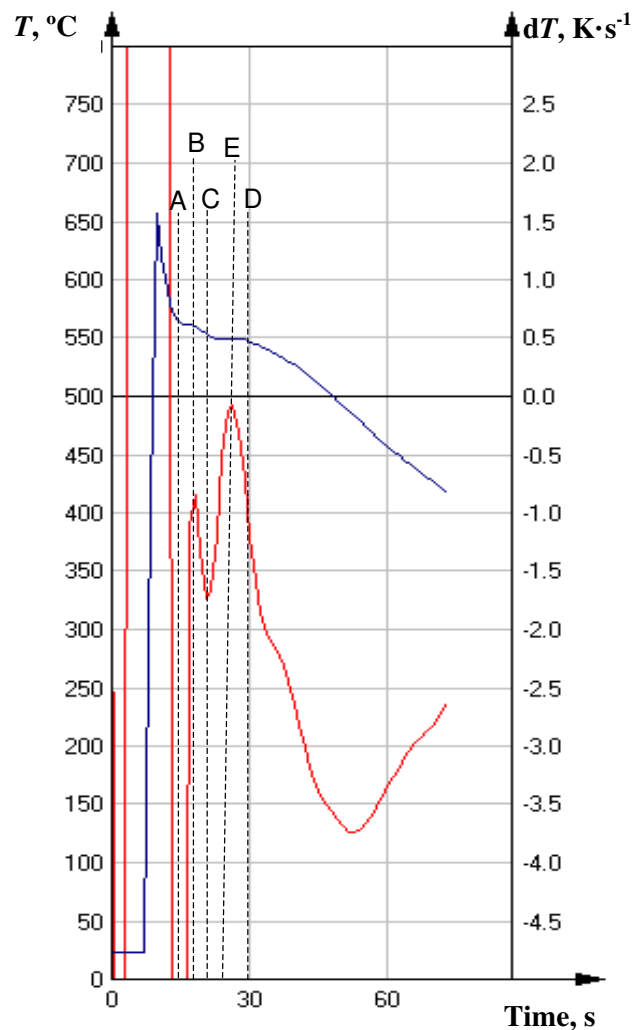


Fig. 6. Cooling curves of AlSi21CuNi alloy with 3 % AlTiB + 1 % Al<sub>3</sub>TiB + 3 % AlTi<sub>6</sub>B:  
 A – occurring of the first nuclei of the  $\beta$  phase, B – maximum thermal effect of  $\beta$  phase crystallization,  
 C – occurring of the end nuclei of the  $\beta$  phase and occurring of the first nuclei of the eutectic ( $\alpha + \beta$ ),  
 D – occurring of the end nuclei of the eutectic ( $\alpha + \beta$ ), E – maximum thermal effect of eutectic ( $\alpha + \beta$ )

Dynamic Scanning Calorimetry curves of heating measurement the AlSi21CuNi alloy with 3 % AlTiB + 1 % Al<sub>3</sub>TiB + 3 % AlTi<sub>6</sub>B for heating rate 5 K·min<sup>-1</sup>, as an example is presented in Fig. 7, and for cooling rate also 5 K·min<sup>-1</sup> is presented in Fig. 8. DSC analysis gives a lot of thermodynamic information showed in Fig. 7 and 8, but applies to small amount of research alloys

(typical measurement samples weight – 10 mg). Measurements can be performed on samples after all treatments, but not in real time of crystallization heats produced in an industrial plant.

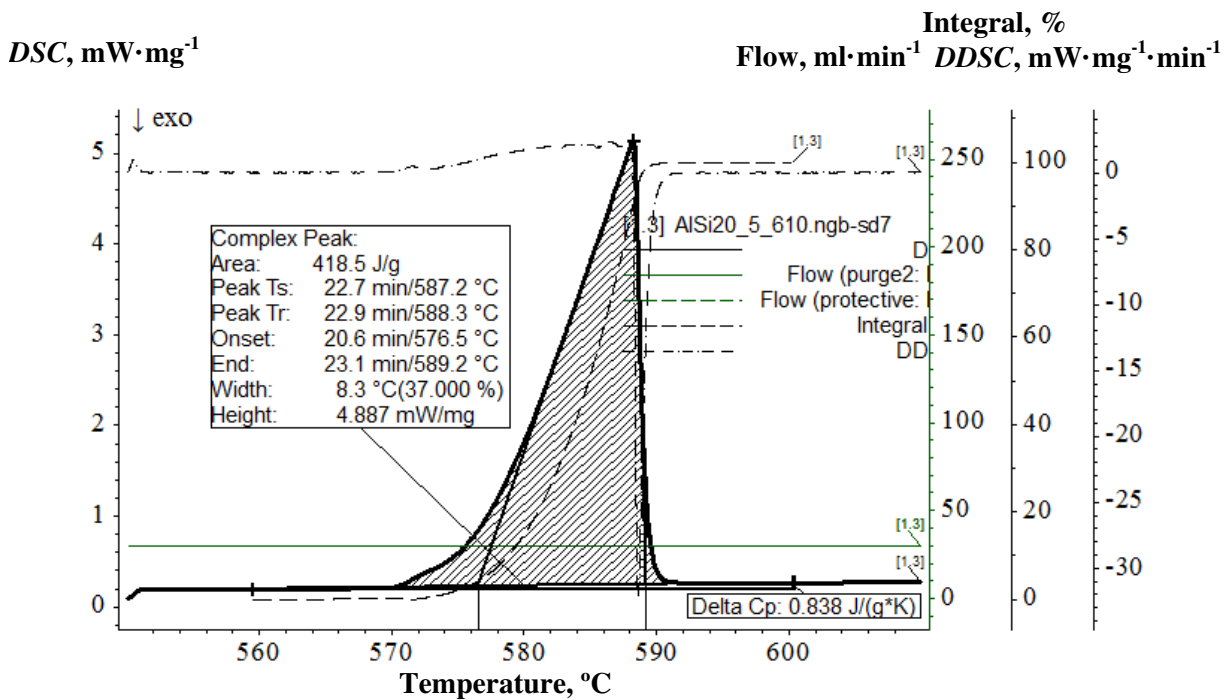


Fig. 7. DSC and DDSC curves of heating measurement the AlSi21CuNi alloy with 3 % AlTiB + 1 % Al<sub>3</sub>TiB + 3 % AlTi<sub>6</sub>B. Heating rate 5 K·min<sup>-1</sup>

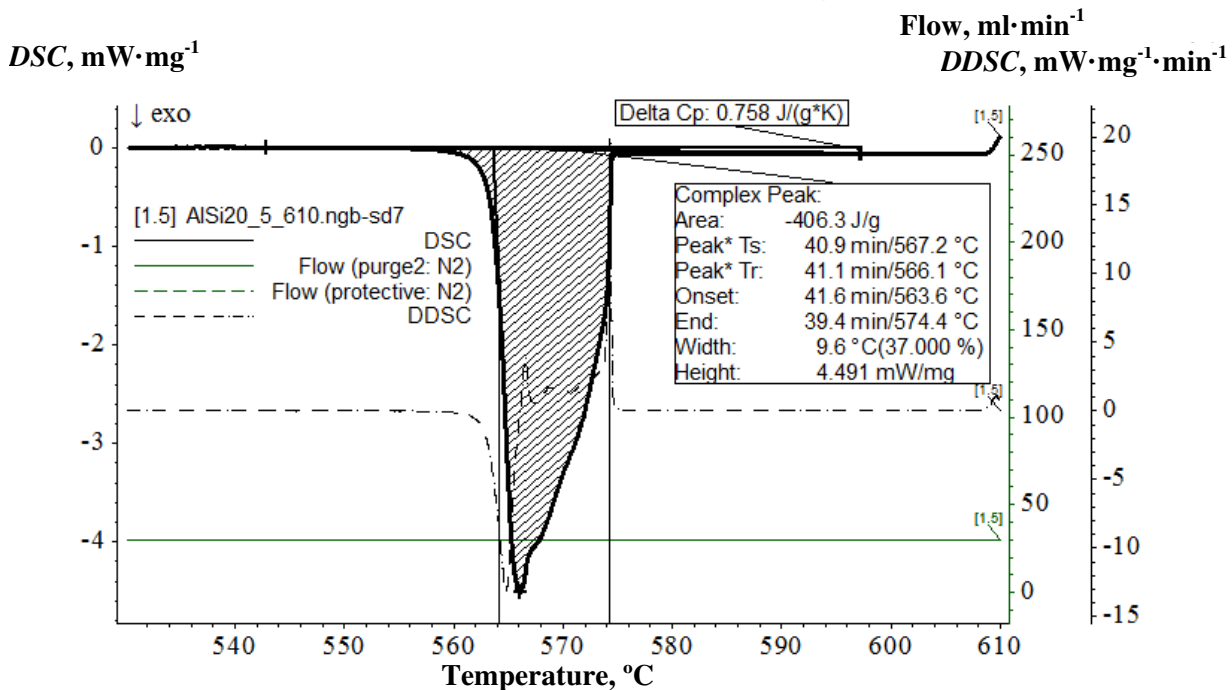


Fig. 8. DSC and DDSC curve of cooling measurement the AlSi21CuNi alloy with 3 % AlTiB + 1 % Al<sub>3</sub>TiB + 3 % AlTi<sub>6</sub>B. Cooling rate 5 K·min<sup>-1</sup>

### Conclusions

1. An analysis of changes in Rm, A and HB values in alloys with a different share of modifiers indicates that the tested chemical additives were characterized by different intensity. The most effective compound was AlTi<sub>6</sub>B (firs of all with AlTiB), followed by AlTiB and Al<sub>3</sub>TiB. The tested compounds' effectiveness was correlated with contents elements of modifier who can be modifiers hyper-eutectic Al-Si alloy.

2. The best results were recorded for a modifying with 3 % AlTiB + 1 % Al<sub>3</sub>TiB + 3 % AlTi<sub>6</sub>B, which enabled to achieve the highest values of all analysing parameters (in this experimental design).
3. DSC measurement is not recommended for determination of modification of alloys produced in an industrial plant.
4. These results suggest the possibility of application of cooling curve and its time derivative curve to determine the modification of alloys.
5. Differential Scanning Calorimetry and conducted experiments that were better understand the relationship between thermodynamic properties, microstructure and mechanical properties of alloys.

## References

1. Hernandez F.C.R, Sokolowski J.H. Thermal analysis and microscopical characterization of Al-Si hypereutectic alloys. *J All Comp.* 419/1, 2006, pp. 180-190.
2. Michna, S., Lukac, I., Ocenasek, V., Koreny, R., Drapala, J., Schneider, H., Miskufova, A. *Encyclopaedia of aluminium*, Adin s.r.o. Presov 2005 (in Czech).
3. Pilarczyk W. The investigation of the structure of bulk metallic glasses before and after laser welding. *Cryst. Res. Technol.* 9-10, 2015, pp. 700-704.
4. Ulewicz R. Quality control system in production of the castings from spheroid cast iron vol. 42, 2003, pp. 61-63.
5. Wołczyński W, Guzik E, Wajda W, Jędrzejczyk D, Kania B, Kostrzewa M. CET in Solidifying Roll – Thermal Gradient Field Analysis, *Arch Metall Mater.* 57/1, 2012, 105-117.
6. Rogal Ł, Dutkiewicz J, Góral A, Olszowska-Sobieraj B, Dańko J. Characterization of the after thixofforming microstructure of a 7075 aluminium alloy gear. *International Journal of Material Forming* vol. 3/1, 2010, pp. 771-774.
7. Grauer S.J., Caron E.J.F.R., Chester N.L., Wells M.A., Daun K.J. Investigation of melting in the Al-Si coating of a boron steel sheet by differential scanning calorimetry. *J Mater Process Tech.* 2016, 2015, pp. 89-94.
8. Lipiński T. Double Modification of AlSi9Mg Alloy with Boron, Titanium and Strontium. *Arch Metall Mater.* Vol. 60, Issue 3b, 2015, pp. 329-333.
9. Lipiński T. Modification of The Al-Si Alloys with the Use of a Homogenous Modifiers. *Arch Metall Mater.* Vol. 53/1, 2008, pp. 193-197.
10. Lipinski T, Szabracki P. Modification of the Hypo-Eutectic Al-Si Alloys with an Exothermic Modifier. *Arch Metall Mater.* Vol. 58/2, 2013, pp. 453-458.
11. Djurdjevic M., Jiang H., Sokolowski J. On-line prediction of aluminum-silicon eutectic modification level using thermal analysis. *Mat Char.* 46, 2001, p. 31-38.
12. Lipiński T., Modification of Al-11 % Si Alloy with Cl – Based Modifier. *Manufacturing Technology* Vol. 15, No. 4, 2015, pp. 581-587.
13. Pilarczyk W, Pilarczyk A. Application of a Control-Measuring Apparatus and Peltier Modules in the Bulk-Metallic-Glass Production Using the Pressure-Casting Method. *Mat Techn.* 49, 2015, pp. 537-541.
14. Náprstková, N., Cais, J., Svobodová, J. The Effect of Modification by Strontium of the AlSi7Mg0.3 Alloy on the Surface Roughness. *Manufacturing Technology*, vol. 13, No. 3, 2013, pp. 380-384.
15. Nová, I., Machuta, J. Squeeze casting results of aluminium alloys. *Manufacturing Technology*, vol. 13, No. 1, 2013, pp. 73-79.
16. Kucharska B., Wróbel A., Kulej E., Nitkiewicz Z. The X-Ray Measurement of the Thermal Expansibility of Al-Si Alloy in the Form of a Cast and a Protective Coating on Steel”, *Sol St Ph.* vol. 163, 2010, p. 286-290.
17. Gašior W., Dębski A., Góral A., Major R. Enthalpy of formation of intermetallic phases from Al-Li system by solution and direct reaction calorimetric method. *J Alloy Compd.* 586, 2014, pp. 703-708.
18. Muhmond H. M., Fredriksson H. An Investigation on the Effect of S and Al on the Austenite Growth Morphology in Gray Cast Iron, Using Thermal Analysis and Etching Technique. *Trans Indian Inst Met* vol. 66(2), 2013, pp. 185-192.